JOURNAL OF MATERIALS SCIENCE 30 (1995) 1719–1727

Fabrication and mechanical properties of *in situ* formed carbide particulate reinforced aluminium composite

H. NAKATA*, T. CHOH, N. KANETAKE
Department of Materials Processing Engineering, School of Engineering, Nagoya University, Furo-cho, Chikusa-ku, 464 Nagoya, Japan

Stable carbide particles of TiC, ZrC and TaC were *in situ* synthesized in liquid aluminium by the reaction between Al–Ti, Al–Zr or Al–Ta systems liquid alloy and SiC or Al_4C_3 particles. It was possible to generate TiC particles of nearly 1 μm diameter, even utilizing SiC of 14 μm. However, the dispersion behaviour of TiC particles in the matrix depended on the size of the raw carbide. Finer SiC made the dispersion of TiC particles more uniform, resulting in a greater improvement of the mechanical properties. Furthermore, although Al–Ti–Si system intermetallic compound was detected in a TiC_p/Al–Si composite fabricated by the melt-stirring method, those compounds considerably decreased in the composite fabricated by the *in situ* method. The mechanical properties of *in situ* formed TiC_p/Al–5 wt% Mg and TiC_p/Al–5 wt% Cu composites were better than those fabricated by the melt-stirring method and by T6 heat treatment, the properties of *in situ* formed TiC_p/Al–5 wt% Cu composite were further improved. The experimental results were analysed by the reaction model based on the assumption that the overall reaction rate was controlled by both the reaction and the diffusion.

1. Introduction

In recent years, much attention has been paid to the development of an effective fabrication process for metal matrix composites. In the *in situ* fabrication process, the spontaneous reaction between the raw materials is utilized to synthesize reinforcements in the metal matrix. Thus it is expected that the *in situ*-formed composites may reveal not only excellent dispersion of fine reinforcing particles, but also high thermodynamical stability.

Sahoo and Koczak [1] reported that the *in situ*-formed TiC_p/Al composites could be fabricated by bubbling carbonaceous gas into the Al–Ti alloy melt yielding excellent mechanical properties even under elevated temperature. However, the process using carbonaceous gas has some practical difficulties, such as the requirement of complicated equipment and problems in controlling the volume fraction of the TiC particle formed. Therefore, a simplified *in situ* process is sought in order to solve these problems.

The present work investigated the fabrication of *in situ*-formed carbide particulate-reinforced aluminium composites by utilizing the reaction between liquid aluminium alloys containing a thermodynamically stable carbide formation element and a relatively unstable carbide such as SiC and Al_4C_3 as the solid carbon source, to improve control of the *in situ* reaction rate and the volume fraction of carbide formed. The dispersion behaviour of particles formed by the *in situ* reaction process, the mechanical properties of *in situ* composites and the mechanism of *in situ* formation of particles in the liquid aluminium alloy were then investigated, and compared with a composite fabricated by the melt-stirring and gas-injection methods.

2. Experimental procedure

Aluminium ingot (99.99%), titanium, zirconium and tantalum particles as carbide formation elements, 99% SiC particles of 0.6, 3 and 30 μm diameter and 99% Al_4C_3 particles of 3, 14 and 30 μm diameter were used as carbon source.

In the first method, 80 g aluminium containing the carbide formation element was melted in an induction furnace in an MgO crucible under an argon atmosphere, and held at the experimental temperatures of 1423, 1473 and 1573 K. Then SiC or Al_4C_3 particles were added and incorporated by the melt-stirring method [2]. During this stirring, TiC, ZrC and TaC particles were formed *in situ* in the liquid aluminium and subsequently the melt was cast into a permanent mould. In part of the experiment, some samples of about 3 g were taken from melt using an alumina-coated

* *Present address*: Toyota Motor Co., Toyota, Aichi, Japan.

0022–2461

quartz tube during stirring in order to investigate the time dependence of the *in situ* reaction by analysing the content of the carbide formation element with an inductively coupled plasma (ICP) emission spectrometric analysis method, and to observe changes in the microstructure of the sample.

The contents of carbide formation elements and the amount of added SiC or Al_4C_3 were determined by the volume fraction of the *in situ*-formed carbide, taking the molar ratio of carbon, supplied through the dissociation of SiC or Al_4C_3, to the carbide formation element, C/Me, to be 0.95 for titanium carbide and 1 for zirconium and tantalum carbides, assuming complete *in situ* reaction.

In the second method, the powder mixture of titanium and Al_4C_3 particles was intermittently added to pure aluminium at the rate of about 1 g/30 s at 1473 K during stirring. After incorporation of all of the added particles, melt stirring was continued for 300 s to complete the *in situ* reaction. The melt temperature was then lowered to 973 K and an alloying element of magnesium or copper was added to produce the Al–5 wt % Mg or Al–5 wt % Cu matrix. Subsequently those samples were solidified in the crucible by air cooling outside the furnace. The amounts of titanium and Al_4C_3 in the powder mixture were determined using the same procedure as in the first method.

The samples fabricated by the first and the second methods were extruded at 773 K with an extrusion ratio of 25. Part of each specimen was machined into a rod having a gauge length of 20 mm and diameter 4 mm, to investigate the mechanical properties; the other part was polished for microstructural studied by SEM, electron probe microanalysis (EPMA) and X-ray diffraction (XRD). SiC_p (nearly 14 μm diameter)/Al–Si and TiC_p (nearly 1 μm)/Al–Si composites were also fabricated by the melt-stirring method at 1073 K with an appropriate stirring time, for comparison with the *in situ*-fabricated composites. The theoretical volume fraction of *in situ*-formed particles reaches 5.5% in the first method, and 5% and 10% in the second method, assuming complete *in situ* reaction.

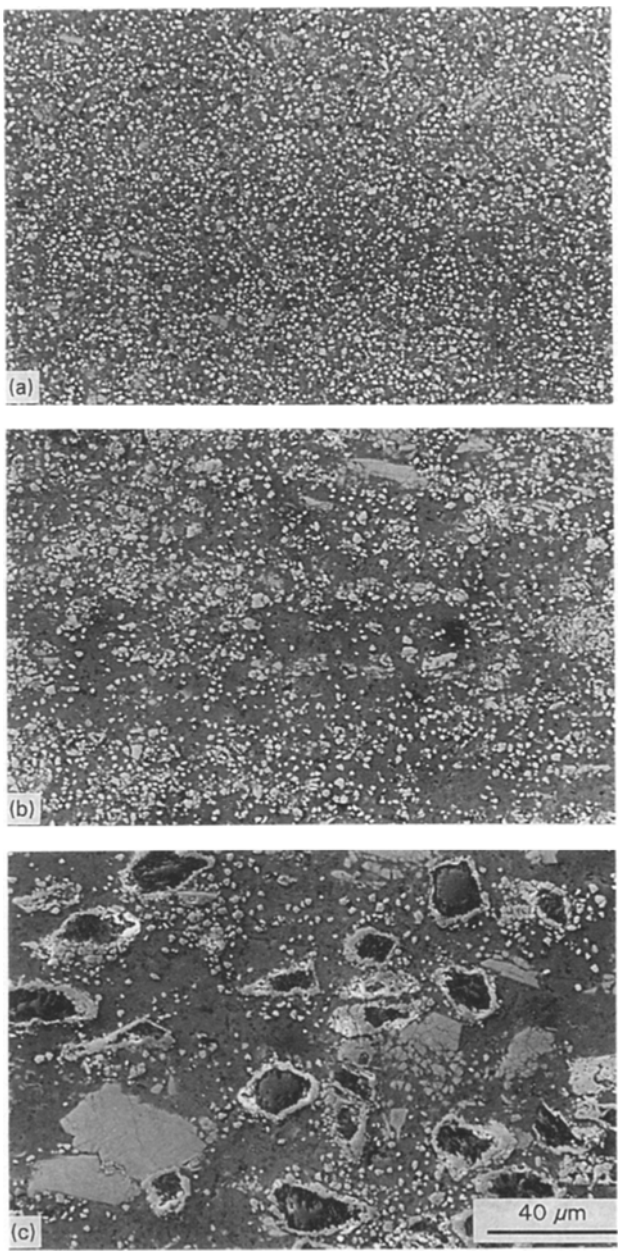

Figure 1 Scanning electron micrographs of *in situ* TiC_p/Al composites fabricated by reaction for 900 s at 1473 K from (a) 0.6 μm, (b) 3 μm, and (c) 14 μm SiC.

3. Results and discussion

3.1. *In situ*-formed TiC particulate-reinforced aluminium composite by the first method

It has been generally reported that SiC particles were poorly incorporated into the melt with decreasing particulate diameter [3]. However, at an elevated melt temperature of 1473 K, fine SiC particles, as small as 0.6 μm diameter, could be incorporated into the melt, because of the essentially improved wettability.

The microstructure of *in situ* composites fabricated from several sizes of SiC particles by the reaction for 900 s at 1473 K are compared in Fig. 1. *In situ* formation of TiC particles was confirmed by XRD and EPMA for the composite shown in Fig. 1a. It is obvious from Fig. 1a that approximately 1 μm or smaller particles are almost uniformly dispersed in the composites fabricated by adding 0.6 μm SiC. The same distribution of *in situ*-formed particles can be achieved when adding 3 μm SiC, as in Fig. 1b. However, using 14 μm SiC particles, as shown in Fig. 1c, the circular TiC phase is observed surrounding the remaining raw SiC particles, due to the decrease in the *in situ* reaction rate, as well as the large intermetallic compounds of Al_3Ti formed from the remaining titanium. Hence, the size of the SiC particle has an effect not only on the rate of the *in situ* reaction, but also on the dispersion behaviour of *in situ*-formed TiC particles. Further, the ultimate tensile strength, the 0.2% proof stress and uniform elongation of those composites were decreased with increasing diameter of SiC, as shown in Fig. 2, depending on this particle dispersion behaviour.

The mechanical properties of *in situ*-formed TiC_p/Al–5 wt % Si composite are compared with those composites reinforced with nearly 14 μm SiC

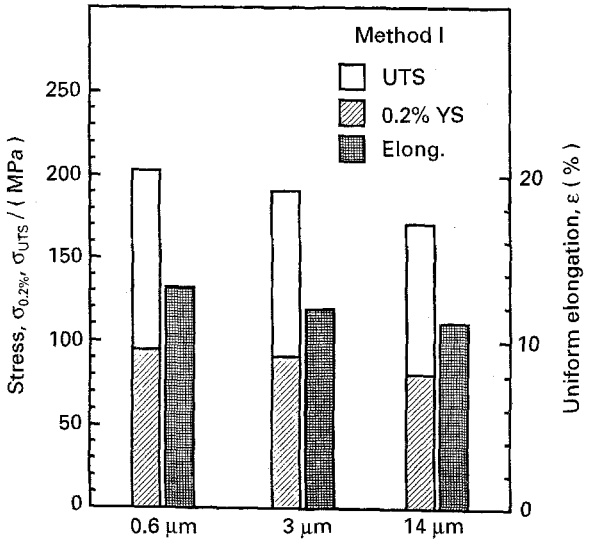

Figure 2 Mechanical properties of *in situ* TiC_p/Al composites fabricated by reaction for 900 s at 1473 K from (a) 0.6 μm, (b) 3 μm, and (c) 14 μm SiC.

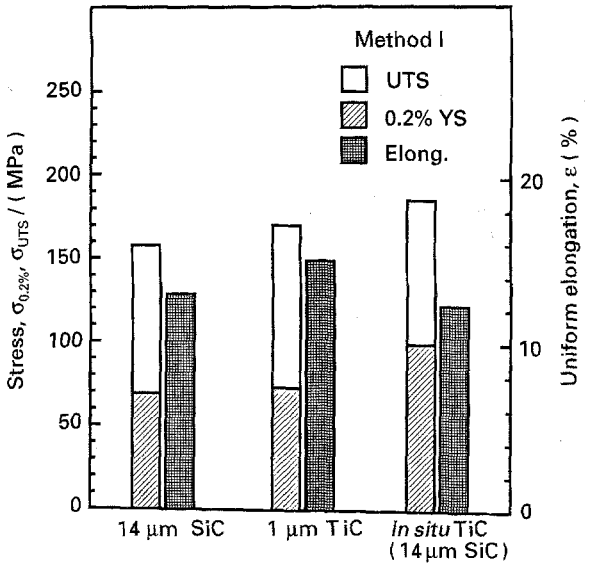

Figure 3 Comparison of mechanical properties of *in situ* TiC_p/Al–Si composites fabricated from 14 μm SiC with those of 14 μm SiC_p/Al–Si and 1 μm TiC_p/Al–Si composites fabricated by the melt-stirring method.

and nearly 1 μm TiC particles fabricated by the melt-stirring method, as shown in Fig. 3. It was found that the ultimate tensile strength and 0.2% proof stress of *in situ* TiC_p/Al–5 wt % Si composite were higher than those of two others fabricated by the melt stirring method, although its uniform elongation was the lowest; i.e. strength efficiency is improved through the *in situ* reaction.

On observing the microstructures of TiC_p/Al–5 wt % Si composites fabricated by both (a) the melt stirring method and (b) the *in situ* method, it should be noted that large precipitates are found in the matrix in the case of the melt-stirring method, as shown in Fig. 4, though the particle size of TiC in both composites is not markedly different. From EDX analysis, those precipitates were found to be Al–Ti–Si system intermetallic compound. This compound may be mainly precipitated through a subsequent process

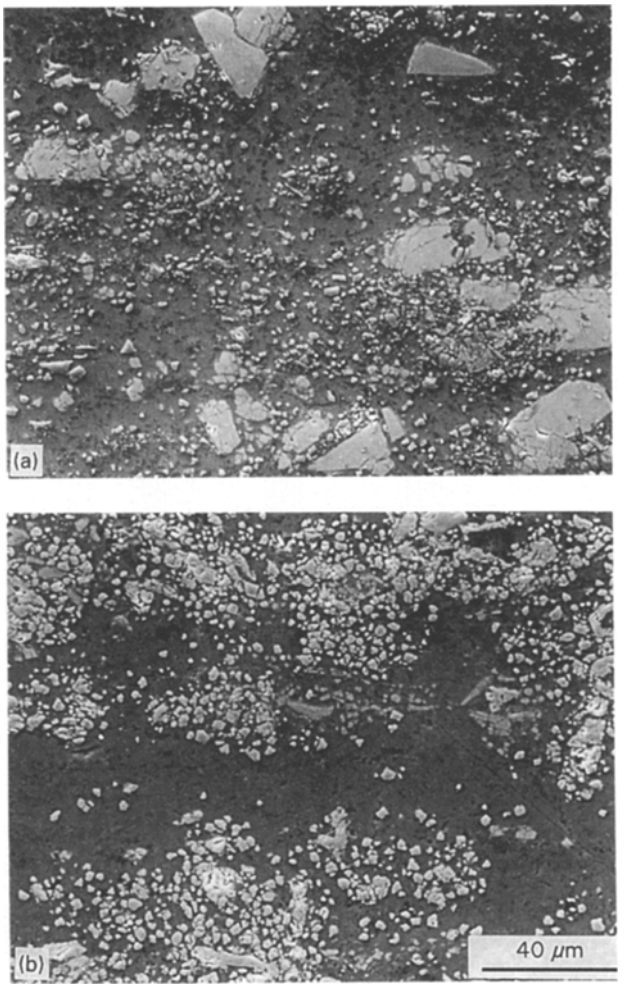

Figure 4 Scanning electron micrographs of TiC_p/Al–5 wt % Si composites fabricated by (a) the melt-stirring method and (b) the *in situ* method.

where titanium and carbon contents are initially increased by the dissolution of added TiC particles then the titanium content reaches its solubility ($3Al + Ti = Al_3Ti$) before the achievement of equilibrium between the titanium content and the carbon content in the liquid aluminium; the precipitation of Al_3Ti then proceeds further until the carbon content in the melt increases to the equilibrium value with the above-mentioned titanium solubility content.

On the other hand, in the matrix of the *in situ* composite, those compounds decreased remarkably. It suggests that the main part of the titanium atoms combine with carbon supplied from SiC, and then the carbon and titanium contents may approach the equilibrium value; during cooling, TiC particles are formed, resulting in a decreasing precipitation of Al_3Ti. Thus the *in situ* composite free from precipitations of Al_3Ti can be fabricated, if the ratio of titanium and carbon contents supplied in the melt is adequate.

3.2. Mechanical properties of *in situ*-formed ZrC and TaC particulate-reinforced aluminium composite

In situ formed ZrC_p/Al and TaC_p/Al composites were fabricated by the first method, adding 14 μm Al_4C_3

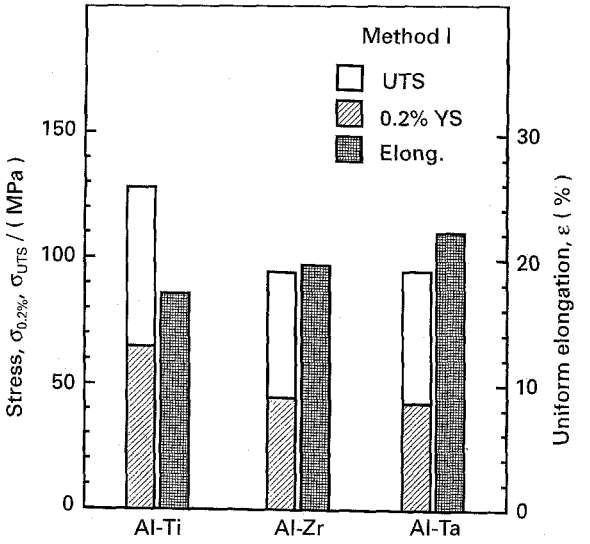

Figure 5 Mechanical properties of *in situ* composites fabricated through the reaction between 14 μm Al_4C_3 particle and Al–Ti, Al–Zr and the Al–Ta system liquid alloys by reaction for 1200 s at 1473 K.

particles to Al–Zr and Al–Ta liquid aluminium alloys and stirring for 1200 s at 1473 K. Fig. 5 shows the mechanical properties of the fabricated composites, compared with those of *in situ*-formed TiC_p/Al composite.

It was found that the ultimate tensile strength and 0.2% proof stress of *in situ* TiC_p/Al composite were the highest, while the highest uniform elongation was obtained in the *in situ* TaC_p/Al composite.

The microstructures of these composites are shown in Fig. 6, where, in the case of *in situ* ZrC_p/Al composite, many unreacted Al_4C_3 particles are found in the matrix with the precipitated intermetallic compound of Al_3Zr and *in situ*-formed circular or flaky ZrC, caused by the slow rate of the *in situ* reaction. On the other hand, in the case of *in situ*-formed TaC_p/Al, fine TaC particles are observed, though they show a more or less agglomerative behaviour. Hence, the strength properties of *in situ* ZrC_p/Al and TaC_p/Al composites are lower than that of TiC_p/Al composite, though their uniform elongations are higher.

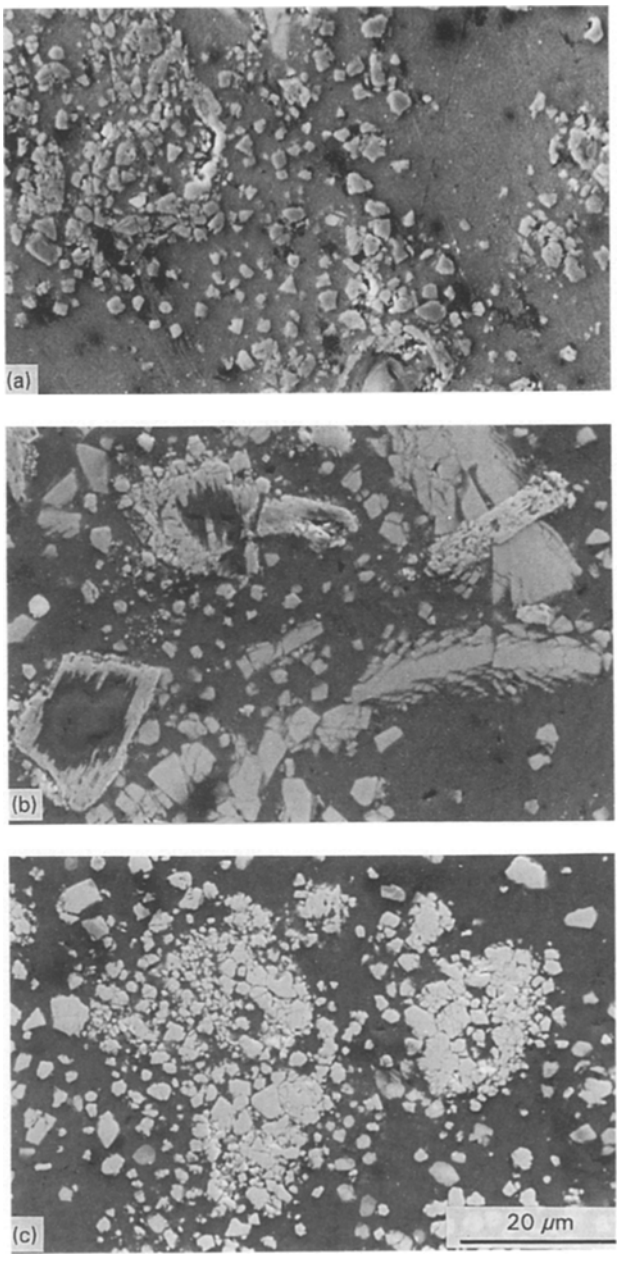

Figure 6 Microstructure of *in situ* composites fabricated through the reaction between 14 μm Al_4C_3 particle and the (a) Al–Ti, (b) Al–Zr and (c) Al–Ta system liquid alloys by reaction for 1200 s at 1473 K.

3.3. The effects of magnesium and copper on the mechanical properties of *in situ* formed TiC_p/Al composite

In situ formed TiC_p/Al–5 wt % Mg and TiC_p/Al–5 wt % Cu composites were fabricated by the second method, where a powder mixture of 3 μm Al_4C_3 and 99% Ti (nearly 350 mesh) was added to the melt at 1473 K in order to increase the volume fraction of the *in situ*-formed particulate reinforcement. After the *in situ* reaction had ceased, magnesium or copper was alloyed at lowered temperature. The values of Young's modulus, ultimate tensile strength and 0.2% proof stress of *in situ* TiC_p/Al–5 wt % Mg composite were increased with increasing volume fraction of *in situ*-formed TiC particles, as shown in Fig. 7. Furthermore, it is noticeable that the ultimate tensile strength and 0.2% proof stress are higher than those obtained in the same composite fabricated by the melt-stirring method, as indicated by the dotted lines [4]. This is contributed to by the better distribution of *in situ*-formed TiC particle in the matrix without the agglomeration of particles.

However, the uniform elongation decreased with increasing volume fraction of TiC_p and, above nearly 10% of volume fraction, became rather less than that obtained by the melt-stirring method.

On the other hand, Fig. 8 shows that Young's modulus, 0.2% proof stress and ultimate tensile strength of the *in situ* TiC_p/Al–4.5 wt % Cu composite also increased and the elongation decreased with increasing volume fraction of TiC_p.

These strength properties were further improved by a T6 heat treatment of 86.4 ks ageing at 450 K after

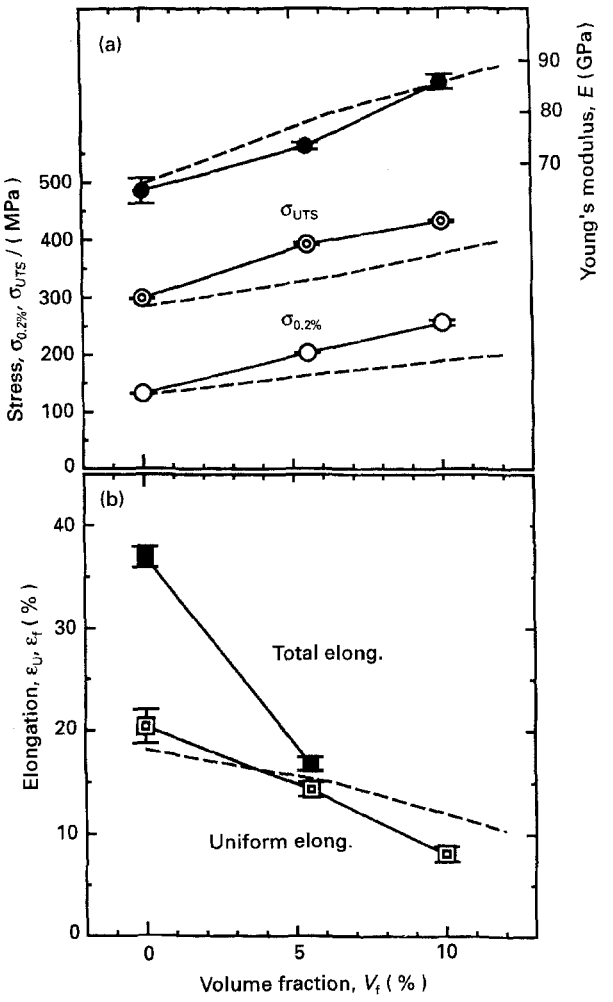

Figure 7 Comparison of mechanical properties of *in situ* TiC_p/Al–5 wt % Mg composites with that (– – –) fabricated by the melt-stirring method [4]. Method II, 3 μm Al_4C_3, T = 1473 K.

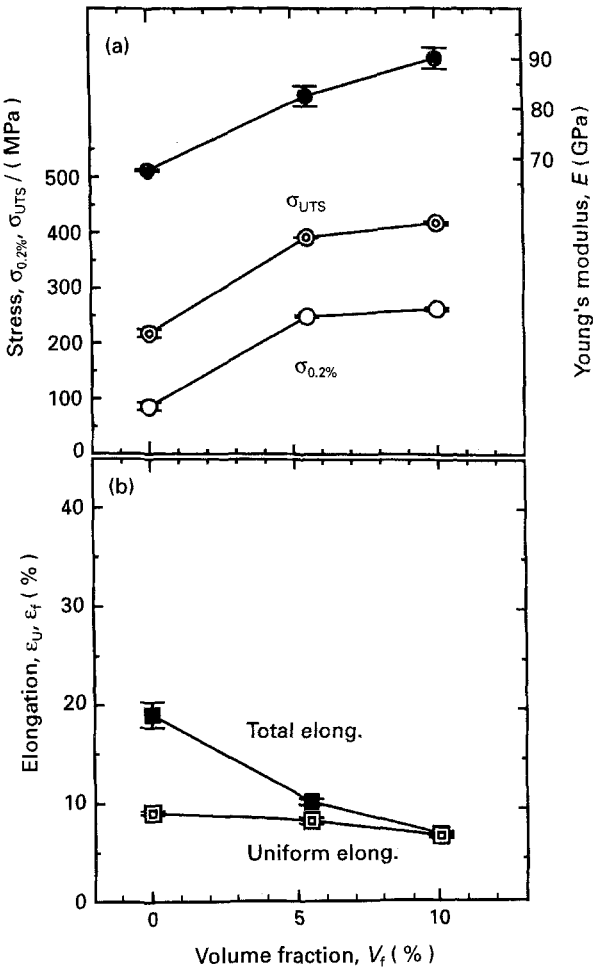

Figure 8 Effect of the particulate volume fraction on the mechanical properties of *in situ* TiC_p/Al–4.5 wt % Cu composite in the as-extruded condition.

the solution heat treatment, as shown in Fig. 9, indicating that the ultimate tensile strength reached 530 MPa at $V_f = 5.5\%$. Moreover, the strengths in the present work are higher than those obtained by the gas-injection method, as indicated by dotted lines [1]. However, the values of ultimate tensile strength and 0.2% proof stress at $V_f = 10\%$ are lower than those at $V_f = 5.5\%$. This may be because of overageing, because although the hardnesses of the matrix and composite at $V_f = 5.5\%$ reached maximum values at about 86 ks ageing, the time required to reach maximum hardness of composite at $V_f = 10\%$ was shortened to about 38 ks. Such acceleration of ageing by reinforcement has been reported in Al–Li [5], Al–Cu–Mg [6] and Al–Mg–Si matrices [7]. Therefore, an ageing time of 86.4 ks is too long for the composite of $V_f = 10\%$, resulting in a decrease in strength.

3.4. Mechanism of *in situ* formation of particles in the liquid aluminium alloys

The mechanism of *in situ* formation of TiC particles was analysed. The time dependence of the behaviour of TiC particles formed *in situ* through the reaction between Al–Ti liquid alloy and 14 μm Al_4C_3 or 14 μm SiC, is shown in Fig. 10, indicating that the *in situ* reaction proceeded leaving the *in situ*-formed TiC particles crowded together in a layer around the raw materials of Al_4C_3 or SiC particles. This suggests that titanium atoms must diffuse in this layer to react with the raw materials. This reaction type is similar to the gaseous reduction of iron oxide pellets, which has been generally analysed by the so-called unreacted core model (e.g. [8]).

Hence, the process of *in situ* formation of particles was analysed by applying the modified unreacted core model, assuming that both *in situ* chemical reaction and titanium diffusion contribute to the overall reaction rate. As shown schematically in Fig. 11, titanium atoms diffuse both in the boundary layer outside the *in situ*-formed TiC particle agglomeration layer and inside its layer, and then reacts with raw carbide.

The diffusion rate of titanium in the boundary layer outside the *in situ*-formed TiC particle agglomeration layer, N_L, is given by

$$N_L = \pi Z_0^2 k_L (C_b - C_{z_0}) \quad (1)$$

where k_L is the mass transfer coefficient ($m\,s^{-1}$).

The diffusion rate of titanium inside the *in situ* formed TiC particle agglomeration layer, N_D, is expressed by Equation 2, taking C_{z_i} ($mol\,m^{-3}$) of

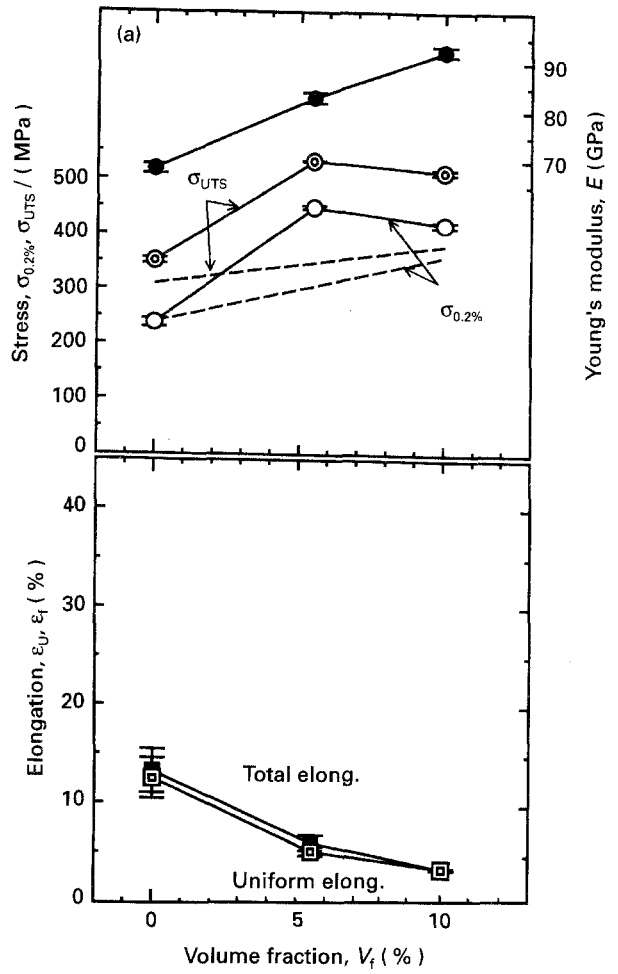

Figure 9 Effect of the particulate volume fraction on the mechanical properties of *in situ* TiC_p/Al–4.5 wt % Cu composite after T6 heat treatment, compared with that (– – –) fabricated by the gas-injection method [1].

titanium content at the plane $Z_i/2$ and D ($m^2 s^{-1}$) of the effective diffusion coefficient into account

$$N_D = \pi Z^2 D(dC_{Z_i}/dZ_i) \quad (2)$$

By integrating Equation 2 from Z_0 to Z, Equation 3 can be obtained

$$N_D = \pi DZZ_0(C_{Z_0} - C_Z)/(Z_0 - Z) \quad (3)$$

The interfacial reaction at the surface of unreacted raw carbide, N_R, is given by Equation 4, considering the driving force $(C_Z - C_e)$

$$N_R = \pi Z^2 k_R(C_Z - C_e) \quad (4)$$

Assuming that those processes proceed in the steady state, the overall rate is described by Equation 5 from Equations 1, 3 and 4

$$N = \frac{\pi Z_0^2}{(1/k_R)(Z_0^2/Z^2) + (Z_0/D)(Z_0 - Z)/Z + (1/k_L)} \times (C_b - C_e) \quad (5)$$

On the other hand, as the consuming rate of raw carbide is the same as the overall rate, it can be expressed by Equation 6, using the carbon content in the raw carbide, δ_0 ($mol\,m^{-3}$)

$$N = -(\pi\delta_0/6)(dZ^3/dt) \quad (6)$$

Further, using particle diameters of Z_0 and Z or titanium contents of C_{b_0} and C_b at initial and time t, the reaction degree, R, is given by

$$R = 1 - (Z/Z_0)^3 = 1 - (C_b/C_{b_0}) \quad (7)$$

From Equations 5, 6 and 7, the rate of the overall reaction is expressed by

$$dR/dt = \{(1/k_R)(1 - R)^{-2/3} + (Z_0/D)[(1 - R)^{-1/3} - 1] + (1/k_L)Z_0\delta_0\}^{-1} 6(C_b - C_e) \quad (8)$$

Now, neglecting $1/k_L$ because of sufficient melt stirring and also the equibrium titanium content, C_e, because it seems small, and substituting Equation 7 into the integrated Equation 8, after converting the units from ($mol\,m^{-3}$) to (at %) by using $f = \rho_{Al}/(100M_{Al})$, $C_b = fC$ and $C_{b_0} = fC_0$ Equation can be obtained

$$(1/K_1)[(C/C_0)^{-2/3} - 1] + (1/K_2)[\ln(C/C_0) + 3(C/C_0)^{-1/3} - 3] = C_0 t \quad (9)$$

where ρ_{Al} is the density of aluminium ($kg\,m^{-3}$) and M_{Al} is the atomic weight of aluminium ($kg\,mol^{-1}$); K_1 and K_2 are given by

$$K_1 = (4fk_R/\delta_0)(1/Z_0) \quad (10)$$

$$K_2 = (6fD/\delta_0)(1/Z_0)^2 \quad (11)$$

The first and the second terms in the left-hand side of Equation 9, respectively, express the contributions of chemical reaction and diffusion. Therefore, assuming low resistance of diffusion, as in the case of a small raw carbide, Equation 9 becomes Equation 12

$$(1/K_1)[(C/C_0)^{-2/3} - 1] = C_0 t \quad (12)$$

Now, Equations 9 and 12 are applied to the experimental results as models I and II. Fig. 12 shows the time dependence of the titanium content in the melt, analysed by the ICP emission spectrometric analysis method. The rate of consumption of titanium at 1473 K by the raw carbide of Al_4C_3 or SiC, increases with decreasing diameter of those carbides. However, in the cases of 3 μm Al_4C_3 and 3 μm SiC, the rates of the initial stage are decreased by poor wettability, due to the smaller diameter [3].

In order to apply model I, the values of K_1 and K_2 were estimated from the values of the intercept and the slope in the plotted relationship between $t/[(C/C_0)^{-2/3} - 1]$ and $[\ln(C/C_0) + 3(C/C_0)^{-1/3} - 3]/[(C/C_0)^{-2/3} - 1]$ obtained by dividing both sides of Equation 9 by $[(C/C_0)^{-2/3} - 1]$. On the other hand, the value of K_1 in model II was obtained from the slope of the linear relationship between $C_0 t$ and $[(C/C_0)^{-2/3} - 1]$. The solid and dotted lines in Fig. 12 show the applied results of Equations 9 and 12 by using previously estimated values of K_1 and K_2. The solid lines well agree with the experimental results, compared with the dotted lines of model II: namely the contribution of diffusion resistance in the *in situ*-formed TiC particle agglomeration layer cannot be ignored.

In the cases of 3 μm Al_4C_3 and 3 μm SiC, the experimental results could be illustrated by taking,

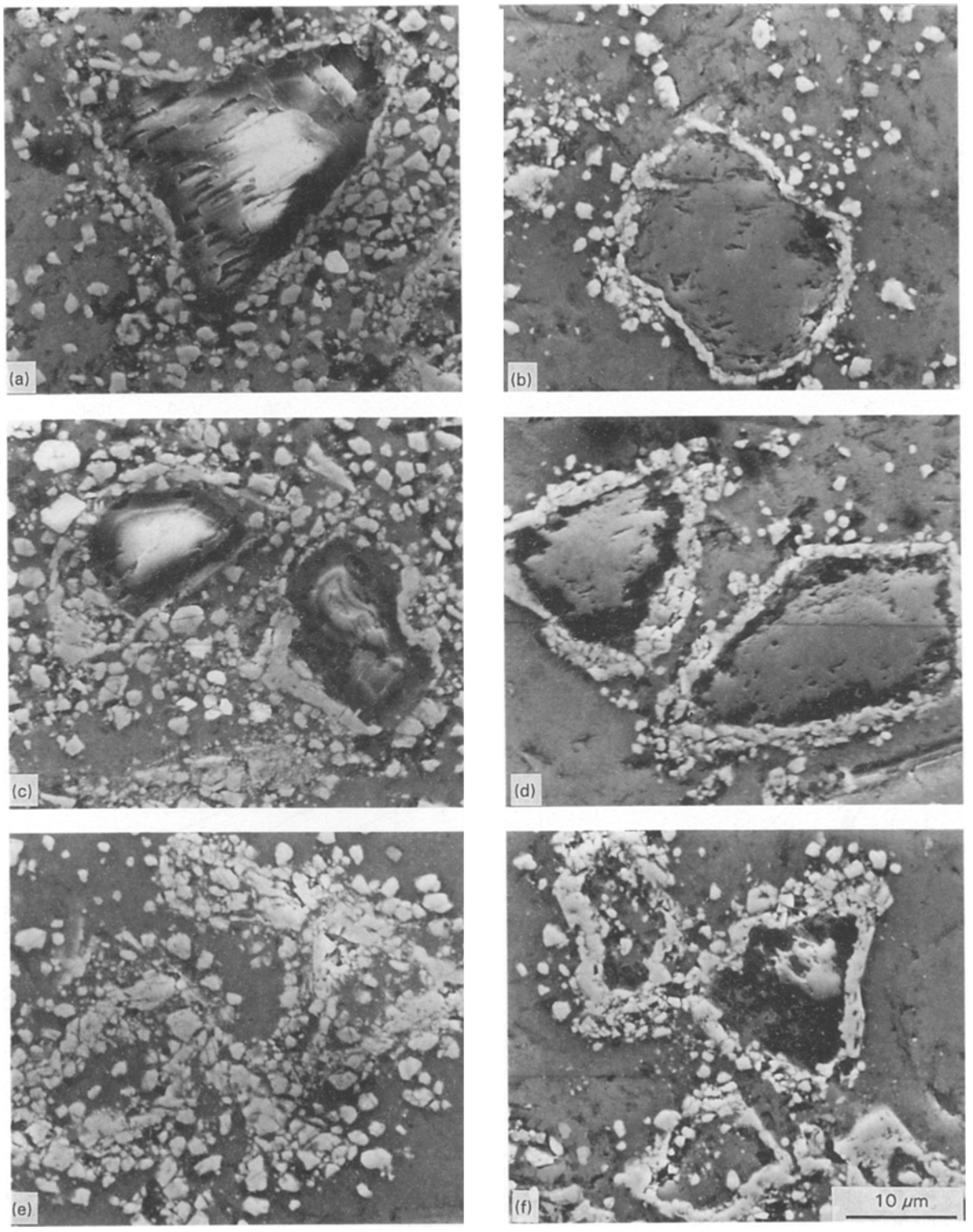

Figure 10 Scanning electron micrographs showing the time-dependence of the behaviour of the titanium carbide formed by *in situ* reaction between (a, c, e) 14 μm Al_4C_3 or (b, d, f) 14 μm SiC and Al–Ti liquid alloy at 1473 K, for (a, b) 150 s, (c) 480 s, (d) 600 s (e, f) 1800 s.

respectively, the incubation times of 300 and 60 s in the initial stage for the incorporation of raw carbide into the liquid aluminium alloy into account [9].

Now, defining two variables of $F_1 = \zeta/(\zeta + \eta)$ and $F_2 = \eta/(\zeta + \eta)$ by expressing the first and second terms on the left-hand side of Equation 9 by ζ and η, those defined values describe the contributions of interfacial chemical resistance and diffusion resistance. As shown in Fig. 13, in the case of the *in situ* reaction system of 14 μm Al_4C_3/Al–Ti, the value of F_1 considerably decreases with time in the initial stage up to nearly 100 s; namely the contribution of the chemical reaction is higher. However, subsequently, the value of F_2 increases remarkably, reflecting the higher contribution of diffusion in the TiC particle agglomeration layer.

Fig. 14 shows the Arrhenius plot for three *in situ* reaction systems of 14 μm Al_4C_3/Al–Ti, 14 μm

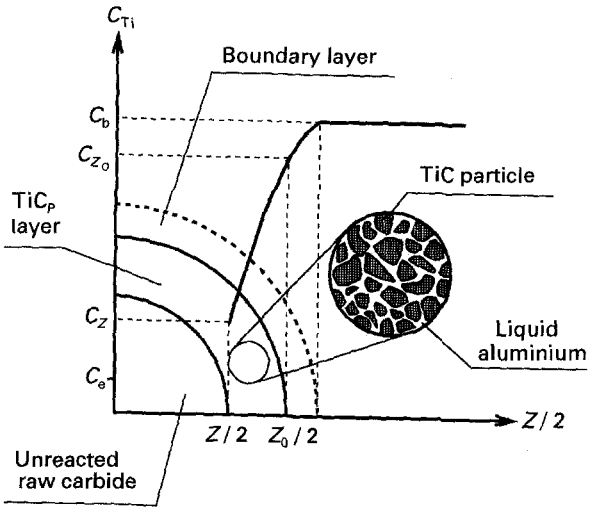

Figure 11 Schematic illustration of the *in situ* reaction model between raw carbide and Al–Ti liquid alloy. (···) the boundary layer; Z_0, Z, diameters of raw carbide at initial and time t (m); C_b, C_e, titanium contents in the melt bulk and equilibrated with TiC (mol m^{-3}); C_{z_0}, C_z, titanium contents at the planes of $Z_0/2$ and $Z/2$ (mol m^{-3}).

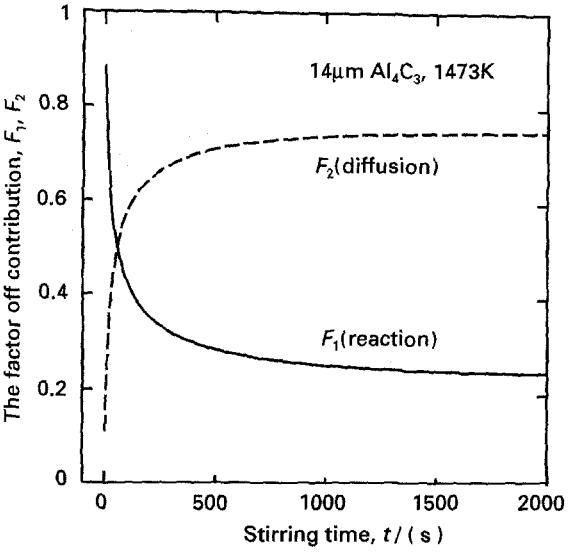

Figure 13 Contributions of chemical reaction, F_1, and diffusion of titanium F_2, in the process of the *in situ* reaction between 14 μm Al_4C_3 and Al–Ti liquid alloy at 1473 K.

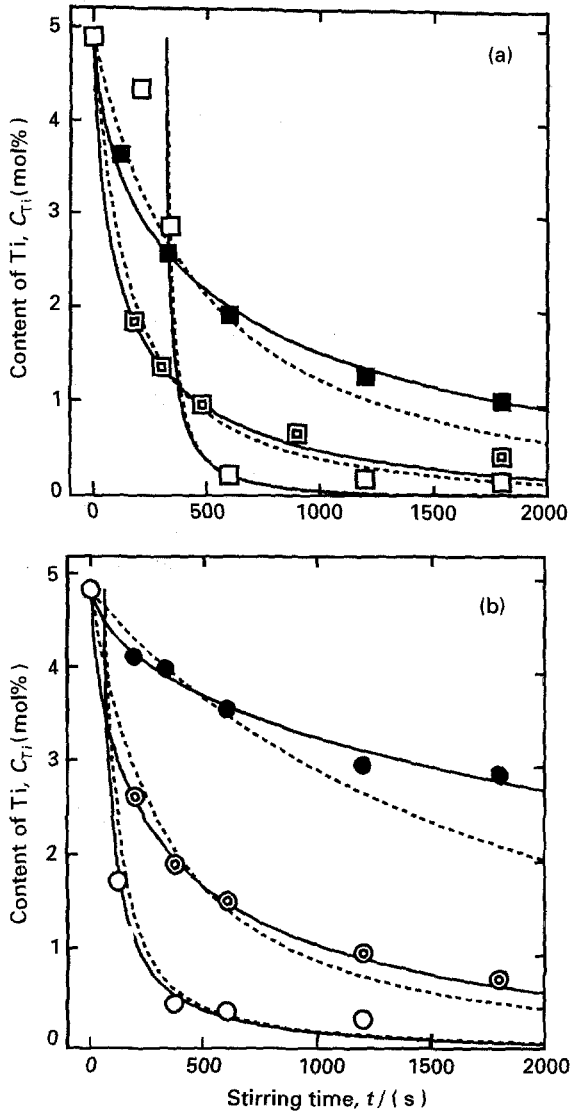

Figure 12 The effects of the initial diameter of raw carbides on the *in situ* reaction rates in (a) Al_4C_3/Al–Ti alloy and (b) SiC/Al–Ti alloy systems, and the applications of models (——) I and (– – –) II. (■, ●) 30 μm, (⊡, ◎) 14 μm, (□, ○) 3 μm.

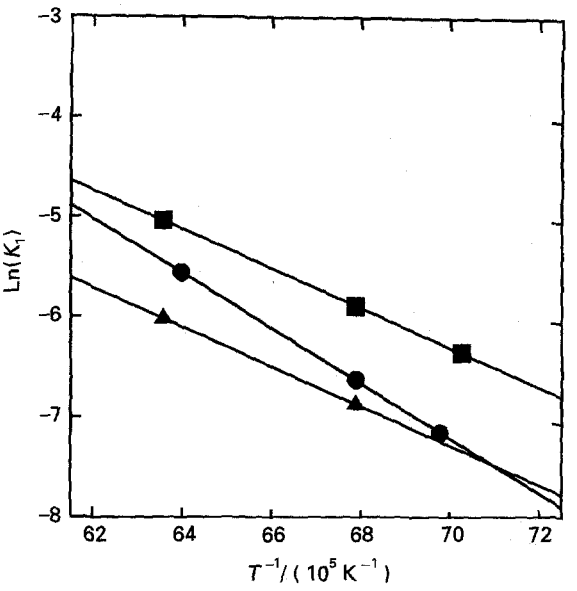

Figure 14 Relation between $\ln K_1$ and $1/T$: $Z_0 = 14$ μm, (■) Al–Ti/Al_4C_3, (▲) Al–Zr/Al_4C_3, (●) Al–Ti/SiC.

Al_4C_3/Al–Zr and 14 μm SiC/Al–Ti. The activation energies obtained from the slopes of the linear lines of the Al_4C_3/Al–Ti and Al_4C_3/Al–Zr systems are similar, 158 kJ mol^{-1}, although that of the SiC/Al–Ti system reaches a higher value, 223 kJ mol^{-1}.

It was previously reported that the value of activation energies of the wetting reaction of SiC and graphite to the liquid aluminium alloy were independent of alloying elements and further that the wetting reaction was consequently limited by the dissociation processes of SiC and graphite [10, 11]. Therefore, it seems likely that, considering that the value of the activation energy of the *in situ* reaction depends similarly only on the kind of carbide, the interfacial chemical reaction is controlled not by the *in situ* reaction for the formation of stable carbide, but by the dissociation of the raw carbides of Al_4C_3 and SiC.

TABLE I Reaction rate constant, k_R, and effective diffusion coefficient, D, estimated from model I

Temp. (K)	System	k_R ($m s^{-1}$)	D ($m^2 s^{-1}$)	Reference
1423	14 μm Al_4C_3/Al–Ti	3.8×10^{-7}	3.2×10^{-13}	
1473	14 μm Al_4C_3/Al–Ti	6.0×10^{-7}	6.2×10^{-13}	
1573	14 μm Al_4C_3/Al–Ti	1.4×10^{-6}	1.7×10^{-12}	
1473	14 μm Al_4C_3/Al–Zr	2.3×10^{-7}	1.2×10^{-13}	
1473	14 μm SiC/Al–Ti	4.6×10^{-7}	3.9×10^{-13}	
1473	Ti in Al(l)/Al	–	2.1×10^{-8}	[12]
1473	C in TiC(s)	–	1.7×10^{-16}	[13]

Table I shows the values of the effective diffusion coefficient, D, and the chemical reaction constant, k_R, obtained from Equations 10 and 11 by using the values of K_1 and K_2 in model I, $\rho_{Al} = 2725 - 0.35T$ ($kg m^{-3}$), $M_{Al} = 2.70 \times 10^{-2}$ ($kg mol^{-1}$), $\delta_0(Al_4C_3) = 4.92 \times 10^4$ $mol m^{-3}$) and $\delta_0(SiC) = 7.80 \times 10^4$ mol m^{-3}), where T is the absolute temperature. The self-diffusion coefficient of titanium in the liquid aluminium at 1473 K, D(Ti in Al) , estimated from the modified Stokes–Einstein equation by Geiger and Poiorier [12], and the diffusion coefficient of carbon in solid TiC, D(C in TiC), calculated from $D(TiC_{0.95}) = 7.6 \times 10^{-5}$ $\exp(-39\,500/T)$ ($m^2 s^{-1}$) [13] are also given in Table I. The value of D of the Al_4C_3/Al–Ti system increases with increasing temperature suggesting a decrease in diffusion resistance in the TiC particle agglomeration layer. Furthermore, the order of D obtained here lies between D(Ti in Al) and D(C in TiC). The result that the *in situ* reaction rate of the SiC/Al–Ti system was lower than that of the Al_4C_3/Al–Ti system, is caused by the decreases in both values of D and k_R due to the lower dissociation rate of SiC, as shown by the higher activation energy in Fig. 14, compared with Al_4C_3.

On the other hand, the value of D in the Al_4C_3/Al–Zr system is lower than that in the Al_4C_3/Al–Ti system, because of the circular dense growth of ZrC phase around the Al_4C_3 particles.

4. Conclusions

In situ-formed carbide particulate-reinforced aluminium composites were fabricated using SiC and Al_4C_3. The mechanical properties, dispersion behaviour of *in situ*-formed particles, and the mechanism of *in situ* formation of the particles were investigated.

1. Fine TiC particles 1 μm in diameter were *in situ* formed even by using 14 μm SiC. However, the finer the raw carbide of SiC and Al_4C_3, the greater was the uniform dispersion of *in situ*-formed particle and the more the mechanical properties of composite were improved.

2. The mechanical properties of the composite fabricated from the Al_4C_3/Al–Ti system were better than those obtained from the Al_4C_3/Al–Zr and Al_4C_3/Al–Ta systems.

3. The mechanical properties of *in situ*-formed TiC_p/Al–5 wt % Mg composite were better than those fabricated by the melt-stirring method, and those properties of the *in situ* formed TiC_p/Al–5 wt % Cu composite after the T6 heat treatment were also better than those fabricated by the gas-injection method.

4. It seems reasonable to consider that the rate of *in situ* carbide formation is controlled by the interfacial chemical reaction during the initial stage, although subsequently it becomes mainly limited by the titanium diffusion in the *in situ*-formed TiC particle agglomeration layer.

References

1. P. SAHOO and M. J. KOCZAK, in Proceedings of the 1st Japan International SAMPE Symposium, edited by N. Igatsa, I. Kinpara, T. Kishi, E. Nakata, A. Ohkura, T. Uriu (SAMPE, Tokyo, 1989) p. 958.
2. M. KOBASHI and T. CHOH, *J. Jpn Inst. Metals.* **55** (1991) 731.
3. T. CHOH, Z. EBIHARA and T. OKI, *J. Japan Inst. Light Metals* **39** (1989) 356.
4. M. KOBASHI, M. HARATA and T. CHOH, *ibid.* **43** (1993) 522.
5. S. HONG, H. TEZUKA and A. KAMIO, *ibid.* **43** (1993) 82.
6. T. CHRISTMAN and S. SURECH, *Acta Metall Mater* **36** (1988) 1691.
7. D. J. TOWLE and C. M. FRIEND, *J. Mater. Sci.* **27** (1992) 2781.
8. K. MORI, *Tetsu-to-Hagane* **50** (1964) 2259.
9. M. KOBASHI and T. CHOH, *J. Jpn Inst. Metals.* **55** (1991) 79.
10. T. CHOH and T. OKI, *Mater. Sci. Technol.* **3** (1987) 378.
11. T. CHOH, R. KAMMEL and T. OKI, *Z. Metallkde* **78** (1987) 286.
12. G. H. GEIGER and D. R. POIORIER, in "Transport Phenomena in Metallurgy", edited by M. Cohen (Addison-Welsey, London, 1973) p. 456.
13. F. J. J. VAN LOO and G. F. BASTIN, *Metall. Trans.* **20A** (1989) 403.

Received 14 April
and accepted 16 September 1994